Article

Novel Lipid Mediator *7S,14R*-Docosahexaenoic Acid: Biogenesis and Harnessing Mesenchymal Stem Cells to Ameliorate Diabetic Mellitus and Retinal Pericyte Loss

Yan Lu , Haibin Tian [*] , Hongying Peng , Nicolas G. Bazan , Song Hong [*]

Article

Novel Lipid Mediator 7S,14R-Docosahexaenoic Acid: Biogenesis and Harnessing Mesenchymal Stem Cells to Ameliorate Diabetic Mellitus and Retinal Pericyte Loss

Yan Lu [1,†], Haibin Tian [1,2,*,†], Hongying Peng [3], Nicolas G. Bazan [1,4] and Song Hong [1,4,*]

[1] Neuroscience Center of Excellence, School of Medicine, L.S.U. Health, New Orleans, LA 70112, U.S.A

[2] Current address: Department of Ophthalmology of Tongji Hospital, Laboratory of Clinical and Visual Sciences of Tongji Eye Institute; School of Medicine; Tongji University, 389 Xincun Road, Shanghai 200065, and Department of Physiology and Pharmacology; TUSM, Shanghai 200092, China

[3] Biostatistics, Department of Environmental Health, University of Cincinnati College of Medicine, Cincinnati, OH 45221, U.S.A

[4] Department of Ophthalmology, School of Medicine, L.S.U. Health, New Orleans, LA 70112, U.S.A

[*] Correspondence: S.H.: shong@lsuhsc.edu; H.T.: Haibin Tian (tianhb@tongji.edu.cn) are co-corresponding authors, who contributed equally to this study.

[†] These authors contributed equally to this work and share first authorship.

Abstract: Stem cells can be used to treat diabetic mellitus and complications. ω3-docosahexaenoic acid (DHA) derived lipid mediators are inflammation-resolving and protective. This study found novel DHA-derived 7S,14R-dihydroxy-4Z,8E,10Z,12E,16Z,19Z-docosahexaenoic acid (7S,14R-diHDHA), a maresin-1 stereoisomer biosynthesized by leukocytes and related enzymes. Moreover, 7S,14R-diHDHA can enhance mesenchymal stem cell (MSC) functions in the amelioration of diabetic mellitus and retinal pericyte loss in diabetic *db/db* mice. MSCs treated with 7S,14R-diHDHA were delivered into *db/db* mice *i.v.* every 5 days for 35 days. Blood glucose levels in diabetic mice were lowered by 7S,14R-diHDHA-treated MSCs compared to control and untreated MSC groups, accompanied by improved glucose tolerance and higher blood insulin levels. 7S,14R-diHDHA-treated MSCs increased insulin⁺ β-cell ratio and decreased glucogan⁺ α-cell ratio in islets, as well as reduced macrophages in pancreas. 7S,14R-diHDHA induced MSC functions in promoting MIN6 β-cell viability and insulin secretion. 7S,14R-diHDHA induced MSC paracrine functions by increasing the generation of hepatocyte growth factor and vascular endothelial growth factor. Furthermore, 7S,14R-diHDHA enhanced MSC functions to ameliorate diabetes-caused pericyte loss in diabetic retinopathy by increasing their density in retina in *db/db* mice. Our findings provide a novel strategy for improving therapy for diabetes and diabetic retinopathy using 7S,14R-diHDHA-primed MSCs.

Keywords: diabetic mellitus and complications; mesenchymal stem cell; 7S,14R-diHDHA; *db/db* mice; blood glucose level; β-cell and α-cell; macrophage; insulin; pancreas and islets; retinopathy

1. Introduction

Type 2 diabetes, accounting for > 90% of diabetes worldwide, is a major public health problem and places a severe economic burden on health care systems. It is characterized by insulin resistance in peripheral tissues. As long as pancreatic β-cells are able to compensate for insulin resistance by enhancing insulin secretion and increasing β-cell mass, euglycemia can be maintained. However, when they are unable to meet the body's demand for insulin because of genetic defects and/or exogenous insults, diabetes mellitus ensues [1–4]. Chronic hyperglycemia leads to glucose toxicity and worsening of impaired insulin secretion due to the overworking of pancreatic β-cells, which results in a decreased ability to secrete insulin. Hyperglycemia can also cause oxidative stress, which influences β-cell survival [5,6]. Reduced β-cell function has been observed in both obese and lean

2

type 2 diabetic humans and in diabetic rodent models [7–11]. Therefore, prevention of the progression of pancreatic β-cell dysfunction in patients with diabetes mellitus should be a key in the long-term management of diabetes mellitus.

Hypoglycemic agents can significantly reduce the development of diabetic complications [12–14]; however, many of them cause adverse effects and sometimes result in progressive deterioration in β-cell function [15–17]. Recently, some strategies using antioxidative treatment have been shown to ameliorate diabetic mellitus. An angiotensin II type 1 receptor blocker was shown to decrease oxidative stress markers in β-cells, improve abnormalities of pancreatic islets in diabetes *db/db* mice [18–20]. Also, increasing levels of the antioxidant enzyme, glutathione peroxidase-1, specifically in β-cells, has been demonstrated to protect them against the adverse effects of chronic hyperglycemia in *db/db* mice [21,22].

Multiple differentiation capacity, paracrine functions, and immunomodulation action make the marrow mesenchymal stem cells (MSCs) a good candidate for prevention or cure of diabetic mellitus and complications [23–26]. Transplantation of bone marrow–derived cells increased levels of serum insulin and reduced blood glucose levels in hyperglycemic mice with streptozotocin-induced pancreatic tissue damage, which improved the metabolic state and survival of recipients [27,28]. Studies using rat MSCs [29,30] or human bone marrow–derived multipotent stromal cells [31–33] have shown similar results of enhanced insulin secretion and repair of pancreatic islets after streptozotocin treatment in rodents. Patients with type 2 diabetes received an intrapancreatic autologous bone marrow stem cell infusion; after 1 year, these patients showed improved metabolic control and reduced insulin requirements [34,35]. However, diabetic hyperglycemia and concomitant oxidative stress damage DNA, proteins, and lipids in various tissues, resulting in dysfunction of cells and enzyme systems. When MSCs are transplanted into diabetes, the inhospitable environment might damage MSC functions [36,37].

Diabetic retinopathy, a secondary microvascular complication of diabetes mellitus, is the leading cause of blindness in the United States among individuals aged 20 to 64 [38,39]. A persistent increase in blood glucose levels shunts excess glucose into the aldose reductase pathway in certain tissues, which converts sugars into alcohol (*e.g.*, glucose into sorbitol, galactose to dulcitol). Pericytes of retinal capillaries seem to be affected by this increased level of sorbitol. Thus, the loss of function of pericytes results in weakness and eventual vascular outpouching of capillary walls, resulting in microaneurysms [38,40].

Docosahexaenoic acid (DHA) is an essential omega-3 fatty acid. Resolvin D series, neuroprotectins, and maresins are potent anti-inflammatory lipid mediators (LMs) naturally generated from DHA during inflammation and/or resolution of inflammation [41–45]. Neuroprotectin D1 and other DHA derived lipid mediators have been reported to protect retinal epithelial cells and neuronal-glial cells from apoptosis induced by oxidative stress [46–49], promote neuronal functions and prevent neural degeneration [50–53]. We identified a DHA-derived LM, 14*S*,21*R*-diHDHA, which promotes wound healing [54–56], inhibits MSC apoptosis, and enhances MSC functions to ameliorate acute kidney injury [57]. In 2009, Serhan *et al.* reported their discovery of maresin 1 (7*R*,14*S*-dihydroxy-4*Z*,8*E*,10*E*,12*Z*,16*Z*,19*Z*-DHA and its inflammation-resolving functions [58]. Inspired by this discovery, we identified and prepared a novel maresin 1 stereoisomer, 7*S*,14*R*-dihydroxy-4*Z*,8*E*,10*Z*,12*E*,16*Z*,19*Z*-DHA (7*S*,14*R*-diHDHA) from leukocytes and related enzyme incubations, as we predicted the therapeutic significance that the biofunction of maresin 1 is conserved in this stereoisomer and that it could promote MSC amelioration of multiple diseases and injuries. Maresins promote the beneficial bioactions of stem cells in the treatment of diseases [59]. Maresin 1 regulates insulin signaling in human adipocytes as well as in adipose tissue and muscle of lean and obese mice [59]. It inhibits hyperglycemia-induced ferroptosis [60]. DHA preserves visual function by maintaining correct disk morphology in retinal photoreceptor cells [61].

Accordingly, we hypothesized that MSCs can protect pancreas β-cells from the damage of diabetic oxidative stress and ameliorate retinal pericyte loss, and biogenic 7*S*,14*R*-diHDHA can induce MSC protective functions. This was further tested to be positive by our studies *in vitro* and by our experiments using *db/db* diabetic mouse model *in vivo*. 7*S*,14*R*-diHDHA was formed by the

cytochrome P450 enzyme and 5-lipoxygenase (5-LOX) in tandem and by leukocytes [58,62–64]. 7*S*,14*R*-diHDHA induced MSC functions in amelioration of diabetes mellitus in *db*/*db* mice by lowering blood sugar and increasing glucose tolerance and blood insulin levels, and decreased the number of macrophages in islets, increasing β-cell viability, density and insulin secretion, and reducing pericyte loss in the retina. 7*S*,14*R*-diHDHA can enhance the MSC secretion of trophic growth factors. Overall, pretreatment of MSCs with 7*S*,14*R*-diHDHA, or related lipid mediators or structural mimics, may offer a new clinical strategy for improved treatment of diabetic mellitus and retinopathy as well as other diabetic complications.

2. Materials and Methods

Reagents

Racemic ±14-hydroxy-4*Z*,7*Z*,10*Z*,12*E*,16*Z*,19*Z*-DHAs (±14-HDHAs or 14*S*/*R*-HDHAs) and 5-lipoxygenase (5-LOX, human recombinant or potato) were supplied by Cayman (Ann Arbor, MI, USA). NaBH$_4$, interleukin (IL)-1β, TNF-α, and *Escherichia coli* lipopolysaccharide (LPS) were supplied by Sigma-Aldrich (St. Louis, MO, USA).

Cells

MSCs were isolated from the bone marrow of *C57BL/6J* mice (8 weeks old, female, Jackson Laboratory), as described in our publications [57]; more than 95% of isolated MSCs were positive for Sca-1 and CD29 based on flow cytometric analysis [54,57,65]. These MSCs possessed adipogenic and chondrogenic differentiation ability. They were cultured in Dulbecco's modified Eagle's medium (DMEM) containing 10% mesenchymal supplement (Stem Cell Technologies, Vancouver, BC, Canada). Cells in passages 7 through 10 were used for the experiments. The Min6 mouse β-cell line (ATCC, Manassas, VA, USA) was cultured in RPMI1640 containing 10% fetal bovine serum (ATCC, Manassas, VA, USA).

Isolation of human neutrophils, monocytes, and lymphocytes

Human samples were managed following protocols approved by the Institutional Review Boards of our institutes. Established procedures were followed [48,66]. Human peripheral blood supplied by the Blood Center (New Orleans, LA, USA) was from a healthy donor who was unknown to us and who had not been on medication for > 2 weeks prior to donation. We centrifuged the blood in sodium citrate (180 g, 10 min, 23°C); then centrifuged the supernatants (1100 g, 15 min, 23 °C). The plasma (the top layer) was removed. We washed the cell pellets with 7 mM EDTA. Neutrophils and mononuclear cells were separated from blood by a Ficoll-Hypaque gradient. We plated mononuclear cells onto plastic dishes to further separate the cells. The cells adhered to the dishes were monocytes, and nonadhered cells were lymphocytes. Neutrophils, monocytes, and lymphocytes prepared were of > 96% purity. Cell viability was > 95% according to trypan blue exclusion.

Biogenesis of novel 7S, 14R-DHA

14*R*-hydroxy-4*Z*,7*Z*,10*Z*,12*E*,16*Z*,19*Z*-DHA (14*R*-HDHA) was prepared from ±14-HDHAs as described in our previous publication [67] and the section below. We then incubated the 14*R*-HDHA (10 μg/incubation) with 5-LOX (3 h, 37°C) to identify the biogenic pathway of the novel maresin-1 stereoisomer, 7*S*,14*R* dihydroxyl DHA, which is expected to be produced by 5-LOX with 14*R*-hydroxyl preserved. A few grains of NaBH$_4$ powder were added at the end of incubation. For cellular generation of 7*S*,14*R*-diHDHA, human leukocytes (6 x 10^6 neutrophils + 5 x 10^5 monocytes + 3 x 10^6 lymphocytes) were incubated (20 min, 37°C) in phosphate-buffered saline (PBS) containing 200 μg 14*R*-HDHA. This ratio of leukocytes resembles the typical leukocyte profile of healthy adults [68,69]. The cells were then stimulated (37°C, 30 min) with inflammatory factors (10 ng/mL TNFα, 10 ng/mL IL-1β, and 100 ng/mL LPS) as described in our previous publication, to promote the biosynthesis of lipid mediators [54,55,67].

Analysis and Isolation of 7S, 14R-diHDHA and of its precursor 14R-HDHA

14*R*-HDHA (> 98% pure) was isolated from purchased ±14-HDHAs using aqueous reversed-phase chiral liquid chromatography (aR chiral LC) coupled to an ultraviolet photo diode array detector and tandem mass spectrometer (aR chiral LC-UV-MS/MS) as we published previously [54,55,67]. The incubations were extracted and then analyzed or fractionated for 7*S*,14*R*-diHDHA. Briefly, A Chiralpak-IA chiral column (150 mm long x 2.1 mm ID x 5 μm, Chiral Tech, West Chester, PA, USA) was used for the aR chiral-LC separation. The mobile phase flowed at 0.2 mL/min, eluted as B (methanol:H$_2$O:acetic acid = 27:73:0.01) from 0 to 1 min, ramped from B:methanol 40:60 to B:methanol 20:80 by 50 min, ramped to methanol by 55 min, and then flowed as methanol. The instrument used included the system of Survey LC-PDA UV-LTQ linear ion trap MS/MS (Thermo Fisher, Waltham, MA, USA) [54,55] and the system of an Agilent 1100 LC system (HPLC-PDA, Agilent Technologies, Santa Clara, CA, USA) and a QTRAP 6500$^+$ quadruple-linear trap MS/MS (Sciex.com, Framingham, MA, USA), with electrospray ionization for both systems [70]. The LC-UV effluents were split at a 1:20 ratio, where 1 portion went into a mass spectrometer that monitored the chromatography of 7*S*,14*R*-diHDHA and 20 portions were fraction-collected manually for the aR chiral LC peak of 7*S*,14*R*-diHDHA. The collected effluents containing 7*S*,14*R*-diHDHA were pooled together and evaporated for solvent removal under vacuum or nitrogen gas blow.

Protocols for the treatment of cells in vitro

MSCs (2 × 10^5) were treated with 7*S*,14*R*-diHDHA (250 nM) for 12 h. The level of VEGF or HGF in supernatant was analyzed using ELISA kits (RayBiotech, Peachtree Corners, GA, USA, and R&D Systems, USA, respectively). Min6 β-cells were cultured to 60%–80% confluence (1.8 × 10^5) in lower chamber of a 24-transwell plate (8 μm pore) pretreated with polylycine overnight. MSCs (3 × 10^4) were cultured in the upper chamber of a 24-transwell pretreated with or without 250 nM 7*S*,14*R*-diHDHA for 4 h. Min6 β-cells and MSCs were cocultured in RPMI1640 for 8 h, and then treated with 100 or 200 μM H$_2$O$_2$ for 10 h. Cell viability was analyzed using the MTT method. Moreover, Min6 β-cells were treated for 4 h with conditioned medium (CM) of MSCs or 7*S*,14*R*-diHDHA-treated MSCs.

Mice

We used 16-week-old female *C57BL/6J* mice and diabetic *db/db* mice (BKS.Cg-m+/+leprdb/J, Strain #:000642) (Jackson Lab, Bar Harbor, ME). Animal protocols were approved by the Institutional Animal Care and Use Committee and Institutional Review Board of Louisiana State University Health Sciences Center, New Orleans, and followed the ARRIVE guidelines [71]. The studies were conducted in a blinded fashion.

Treatment procedures in vivo

MSCs were cultured with or without 250 nM 7*S*,14*R*-diHDHA for 4 h and then collected trypsinization (0.25% trypsin/0.53 mM ethylenediaminetetraacetic acid; Invitrogen, Carlsbad, CA), similar to the procedures that we used previously [57]. MSCs (1 × 10^6) with or without treatment of 7*S*,14*R*-diHDHA were infused into 16-week-old *db/db* mice via tail vein every 5 days for 35 days. During the intervention period, body weight was measured every week. Nonfasting blood glucose was measured using a OneTouch Ultra glucose meter (LifeScan, Milpitas, CA) every week. The intraperitoneal glucose tolerance test (IPGTT) was conducted as follows. After 5 weeks of treatment, mice were injected intraperitoneally with glucose (2 g/kg body weight) after 8 h of fasting. Blood samples were taken at 0, 60, and 120 min from the tail vein, and blood glucose was measured. Sera were collected at 120 min, and insulin concentrations were measured using ELISA using mouse insulin as a standard.

Histological study

Mice were perfused with PBS at the end of the treatment. Pancreas and eyes were collected and fixed in 4% paraformaldehyde for 2 h, and cryosections (5 μm) were prepared. Sections were blocked

with normal goat serum (10% in PBS) for 30 min at room temperature, and then incubated with the following primary antibodies: rabbit antimouse insulin, rabbit antimouse glucagon, rat antimouse F4/80 (Santa Cruz Biotechnology, Dallas, Texas, USA), and rabbit antimouse α-SMA (Millipore, Burlington, MA, USA). Primary antibodies were followed by incubation with the secondary antibodies: Cy3-labeled goat antirat immunoglobulin G (IgG), Cy5-, or fluorescein isothiocyanate (FITC)-labeled goat antirabbit IgG (Invitrogen, Carlsbad, California, USA). Normal rat IgG and rabbit IgG (Santa Cruz Biotechnology, Dallas, Texas, USA) were used as isotype controls. Nuclei were counterstained with Hochest 33342 (Invitrogen, Carlsbad, California, USA). To assess the α cell ratio, the image analysis software NIH ImageJ was used to calculate the pancreatic islet cell number, the insulin$^+$ and glucagon$^+$ cells in the pancreatic islets to determine the percent β-cell count and α-cell count (relative to the pancreatic islets). The macrophage infiltration in the pancreas was assessed using the number of F4/80$^+$ cells per hpf. To assess retinal pericyte loss, retinal sections were stained with an antibody against α-SMA, which specifically marks pericytes in the capillaries. The number of α-SMA$^+$ cells in the inner nuclear layer of the retinas was counted and normalized against the area of the inner nuclear layer.

Statistical analysis

All data were analyzed using one-way analysis of variance followed by Fisher's least significant difference post hoc test and expressed as mean ± standard error of the mean. $p < 0.05$ was considered statistically significant.

3. Results

3.1. Biogenesis of novel 7S,14R-dihydroxy-4Z,8E,10Z,12E,16Z,19Z-DHA

14R-HDHA forms from DHA by P450 enzymatic conversion, as we observed previously [67]. We predicted that 5-LOX or 5-LOX rich leukocytes [58,62–64] convert 14R-HDHA to 7S,14R-dihydroxy-4Z,8E,10Z,12E,16Z,19Z-DHA where the chirality of C-14 is preserved as 14R, and the C-7 takes in the hydroxyl at S-configuration based on the well-established knowledge of 5-LOX [58,62–64]. This prediction was tested positive as we observed 7S,14R-diHDHA as a single aR-chiral LC peak at 50.6 min (Figure 1A), with its UV spectral triplet possessing a head at 270 nm and two shoulders at 261 and 281 nm representing its conjugated triene (Figure 1B) and its MS/MS spectrum at m/z 359 [molecular mass M-H]$^-$ finger-printing its 7S,14R and double-bond locations (Figure 1C). The MS/MS ions m/z 359 [M-H]$^-$, 341 [M-H-H$_2$O]$^-$, 323 [M-H-2H$_2$O]$^-$, 315 [M-H-CO$_2$], 297 [M-H-H$_2$O-CO$_2$]$^-$, and 279 [M-H-2H$_2$O-CO$_2$]$^-$ were consistent with one carboxyl and a molecular weight (M) of 360 Daltons. The fragment ions m/z 217, 141, 123 [141-H$_2$O]$^-$, and 113 showed a hydroxyl at the 7 position (C$_7$). The fragment ions m/z 221, 203 [221-H$_2$O]$^-$, and 177 [221-CO$_2$]$^-$, demonstrated another hydroxyl at the 14 position (C$_{14}$). These data and our previous observation on P450 formation of 14R-HDHA [67] support our prediction that P450 or 5-LOX act together, generating 7S,14R-diHDHA.

Leukocytes are major blood cells that are essential not only in immunity against infection but also in the protection against or repair of organ degeneration and dysfunction caused by injury, diabetic complication, aging, or other adverse conditions. This is demonstrated by leukocyte production of prohealing resolvins, maresins [58], and/or 14,21-diHDHAs [55,72,73]. To further test our first hypothesis, we incubated human leukocytes (monocytes + neutrophils + lymphocytes) in 14R-HDHA containing medium as we conducted previously [54], then activated the cells with factors involved in inflammation and organ degeneration. The incubations were then studied using aR chiral LC-UV-MS/MS. 7S,14R-diHDHA was found to be the peak at the chromatographic retention time (RT) of 50.7 min (Figure 1D) with UV and MS/MS spectra (Figure 1E and 1F, respectively) matching those of 7S,14R-diHDHA generated by 5-LOX from 14R-HDHA (Figure 1). Of note, a small peak at RT 49.7 min was found to be a 7,14-diHDHA because its UV and MS/MS spectra match those of 7S,14R-diHDHA in Figure 1E and F. This 7,14-diHDHA is generated from added 14R-HDHA as purified leukocytes alone without feeding exogenous substrate did not show detectable 7,14-diHDHA; its 14-hydroxyl should be 14R-hydroxyl because the chirality of its 14-hydroxyl is

preserved when undergoing such enzymatic conversion. It had RT 49.7 min, shorter than 50.7 min of 7*S*,14*R*-diHDHA, thus, its 7-hydroxyl should be 7*R* because the aR chiral LC RT is shorter for a fatty acid derived *R*-hydroxyl compound than for its *S*-epiomer when other structural features are the same (Figure 1A) on the basis of our extensive studies and publications from others [74,75]. The 7*R*-hydroxylation is likely to be catalyzed by P450 enzyme(s) in the leukocytes because P450 can catalyze both *R* and *S* hydroxylation. The exact mechanism of this unknown aspect is beyond the scope of this study. In brief, 7*S*,14*R*-diHDHA was the major product, and 7*R*,14*R*-diHDHA was the minor one when feeding leukocytes with 14*R*-DHA. These results and our previous finding that P450 converts DHA to 14*R*-HDHA converged to the biogenic pathway depicted in Figure 1G that human leukocytes produced 7*S*,14*R*-diHDHA, while cell-possessed P450 and 5-LOX catalyzed the biosynthesis.
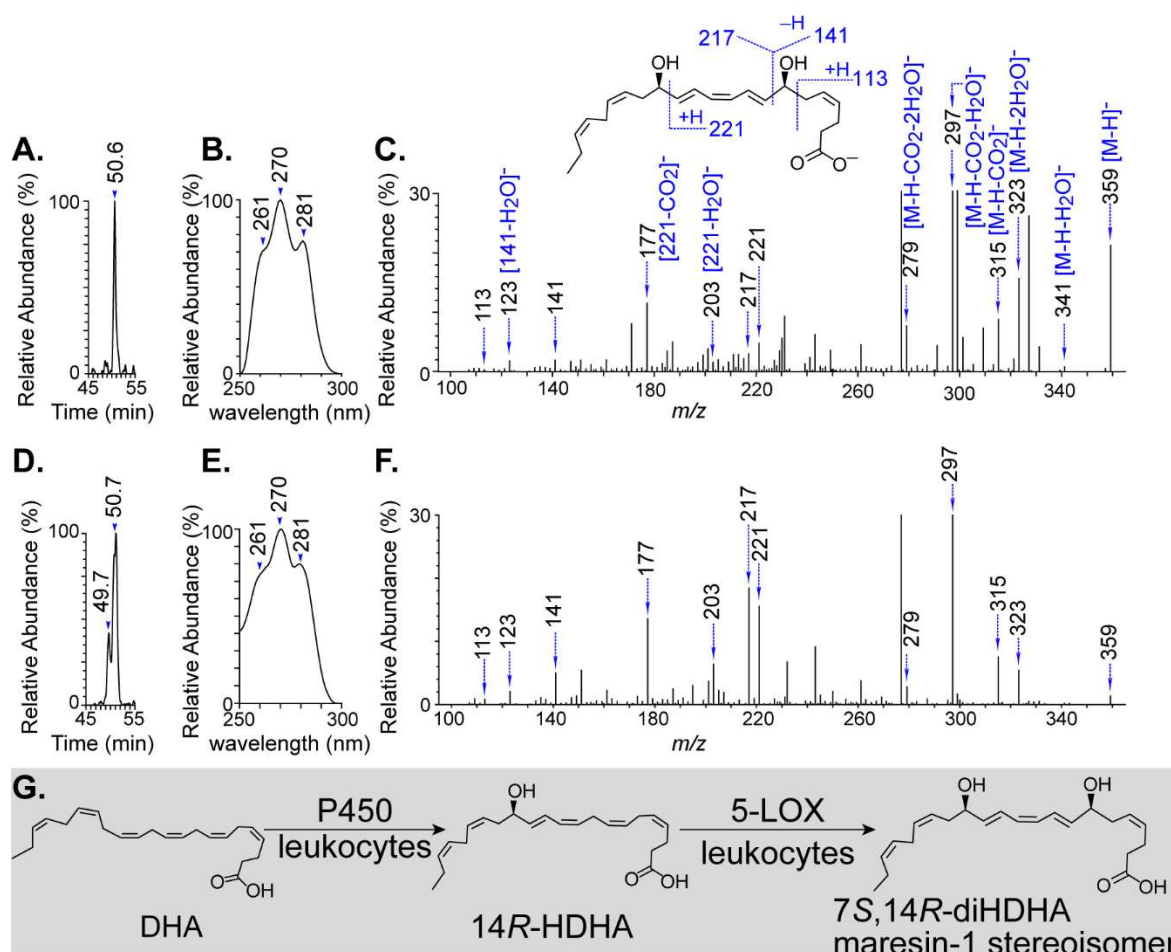

Figure 1. Novel 7*S*,14*R*-dihydroxy-4*Z*,8*E*,10*Z*,12*E*,16*Z*,19*Z*-DHA produced from 14*R*-hydroxy DHA by 5-lipoxygenase or activated human leukocytes. **(A)** Representative aR chiral LC-MS/MS Chromatogram. **(B)** UV spectrum of the flowing chromatographic peak in (A). **(C)** MS/MS spectrum and fragment ion interpretation of the chromatographic peak in (A). **(D)** Representative aR chiral LC-MS/MS Chromatogram. **(E)** UV spectrum of the flowing chromatographic peak in (D). **(F)** MS/MS spectrum and fragment ion interpretation of the chromatographic peak in (D). **(G)** Tentative biogenic pathway for 7*S*,14*R*-diHDHAformation. 7*S*,14*R*-diHDHA was produced by the incubation of 14*R*-hydroxy DHA and 5-lipoxygenase (3 h, 37°C) for (A to C). It was also produced by the incubation of human leukocytes (6 x 10^6 neutrophils + 5 x 10^5 monocytes + 3 x 10^6 lymphocytes) in PBS containing 200 µg 14*R*-HDHA [cultured for 20 min then stimulated by inflammatory factors (10 ng/mL TNFα, 10 ng/mL IL-1β, and 100 ng/mL LPS) for 30 min, 37°C]. The incubation was extracted and analyzed using aR chiral LC-UV-MS/MS as described previously.

3.2. 7S,14R-diHDHA enhanced MSC function to regulate nonfasting blood glucose levels

The *db/db* mice began to exhibit obesity by 5 weeks of age, and body weight increased rapidly with age [9]. 16-week old *db/db* mice weighed twice as much as the control *C57BL/6J* mice (45.3 ± 1.7 vs. 22.3 ± 0.7 g, $p < 0.05$, Figure 2A). The weight of non-diabetic control mice increased a little from 16 to 21 weeks old (Figure 2A). In addition, treatment with MSCs or 7S,14R-diHDHA-treated MSCs had no influence on weight (Figure 2A). The nonfasting blood glucose levels in *db/db* mice were much higher than in normal control *C57BL/6J* mice (640.0 ± 21.4 vs. 120.7 ± 9.3 mg/dL, $p < 0.05$, Figure 2B). At the end of intervention, the blood glucose level did not change in MSC infusion groups, but infusion of 7S,14R-diHDHA-condictioned MSCs reduced the blood glucose level compared to the untreated MSC group (Figure 2B). Blood insulin concentration analysis revealed increased blood insulin levels in the MSC group. Moreover, 7S,14R-diHDHA augmented the MSC effect on insulin secretion (Figure 2C), thus demonstrating that 7S,14R-diHDHA improved MSC amelioration of type 2 diabetic mellitus.
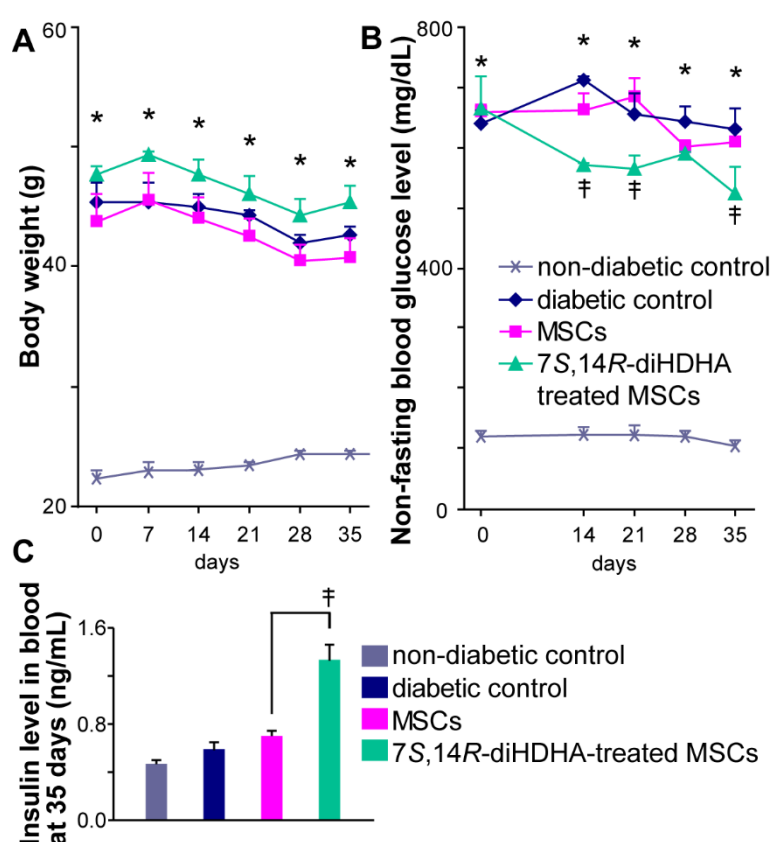

Figure 2. 7S,14R-diHDHA enhanced MSCS function to regulate blood glucose levels. *C57/BL6J* MSCs (1×10^6) with or without treatment of 7S,14R-diHDHA were infused into *db/db* mice via tail vein every 5 days for 35 days. **(A)** Body weight. **(B)** Nonfasting blood glucose levels. **(C)** Blood insulin levels were measured at the end of treatment (35 d). Data are mean $\pm$ SEM, n = 6. *$p < 0.05$ vs. nondiabetic control, ‡$p < 0.05$ vs. MSCs alone.

3.3. 7S,14R-diHDHA treatment promoted the capacity of MSCs to improve glucose tolerance in db/db mice

IPGTT was performed to determine the effect of the treatments of MSCs and 7S,14R-diHDHA-treated MSCs on glucose tolerance. The blood glucose concentration at 120 min after glucose load was significantly reduced by MSC treatment (1078.0 ± 23.4 vs. 1290.0 ± 12.2 mg/dL, $p < 0.05$, Figure 3). In addition, 7S,14R-diHDHA-treated MSCs were more effective than untreated MSCs in reducing glucose concentration (667.0 ± 66.8 *vs*. 1078.0 ± 23.4 mg/dL, $p < 0.05$, Figure 3). These results suggest

that the improvement of glucose tolerance by MSCs and 7S,14R-diHDHA-treated MSCs was at least in part due to improvement of β-cell function.
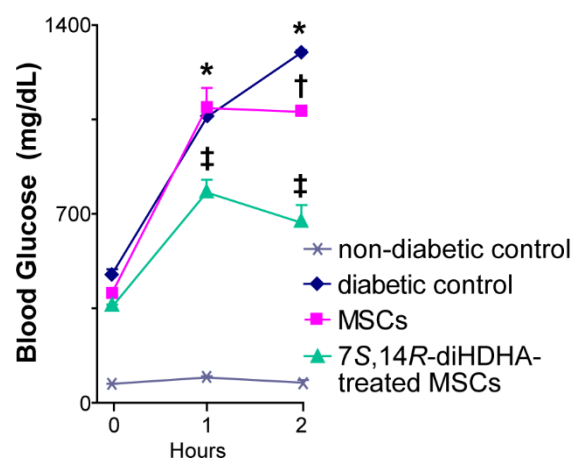

Figure 3. 7S,14R-diHDHA enabled MSCS to promote glucose tolerance in *db/db* mice**.** *C57/BL6J* MSCs (1 × 10^6) with or without treatment of 7S,14R-diHDHA were infused into *db/db* mice via tail vein every 5 days for 35 days. Mice were then injected with glucose (*i.p.,* 2 g/kg body weight) after 8 h of fasting. Blood samples were taken at 0, 1, and 2 h from the tail vein, and blood glucose was measured. Data are mean ± SEM, n = 6. *$p < 0.05$ vs. nondiabetic control; †$p < 0.05$ vs. diabetic control; ‡ $p < 0.05$ vs. MSCs.

3.4. 7S,14R-diHDHA induced MSC function to augment the ratio of β-cells and to reduce the ratio of α-cells in pancreatic islets

Figure 4 shows typical immunostaining patterns of pancreatic islet tissues in the nondiabetic normal *C57BL/6J* mice, diabetic *db/db* mice, and diabetic *db/db* mice infused with MSCs treated with or without 7S,14R-diHDHA. The islet of *C57BL/6J* mice, β-cells occupied most parts of the islets and existed at the center, whereas α-cells existed peripherally. However, *db/db* mice generally have hypertrophied pancreatic islets with a mixture of β-cells and α-cells in the islets. In addition, the ratio of β-cells to total islet cells in a pancreatic islet of *db/db* mice is less than that in *C57BL/6J* mice. Although MSC and 7S,14R-diHDHA-treated MSC infusions cannot change the distribution of β-and α-cells in the islets of *db/db* mice, MSC treatment can increase β-cell ratio compared with diabetic control mice (73.3 ± 1.4% vs. 67.8 ± 2.8%, $p < 0.05$, Figure 4), and 7S,14R-diHDHA can enhance MSC function to augment this ratio (78.2 ± 1.8% vs. 73.3 ± 1.4%, $p < 0.05$, Figure 4). In addition, 7S,14R-diHDHA can enhance MSC function to reduce α-cell ratio in islets of *db/db* mice (Figure 4).
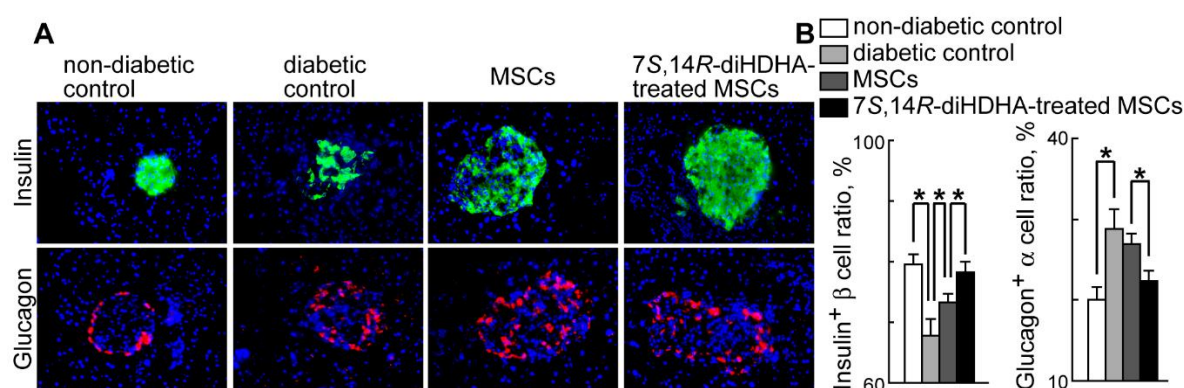

Figure 4. 7S,14R-diHDHA-treated MSCs regulated morphological changes in pancreatic islets. *C57/BL6J* MSCs (1 × 10^6) with or without treatment of 7S,14R-diHDHA were infused into *db/db* mice via tail vein every 5 days for 35 days. Pancreas was collected for histological study. **(A)** Representative pancreatic sections showed insulin$^+$ β-cells (green), glucagon$^+$ α-cells (red) (magnification 200x), and

nuclei were counterstained with Hochest 33342; **(B)** quantification of β-cell ratio and α-cell ratio in islets (n = 60). The results are mean ± SEM. * *p* < 0.05.

3.5. 7S,14R-diHDHA enhanced MSC function to decrease the number of macrophages in islets.

Massive macrophage infiltration was observed in the islets of *db/db* mice compared to *C57BL/6J* mice, which suggests that inflammation may contribute to the dysfunctions of β-cells. In MSC-treated *db/db* mice, the number of macrophages in islets was reduced compared with nontreated *db/db* mice (Figure 5). Treatment with 7*S*,14*R*-diHDHA improved the anti-inflammatory action of MSCs.
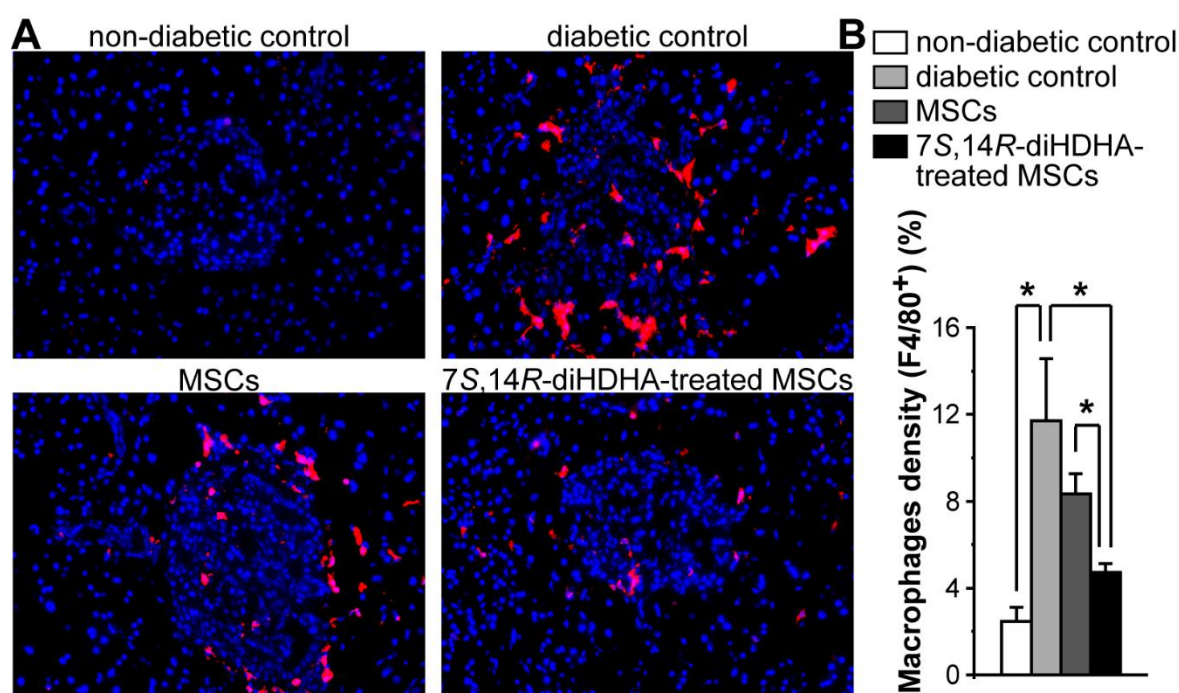

Figure 5. 7*S*,14*R*-diHDHA enhanced MSC function to reduce macrophage accumulation in islets. *C57/BL6J* MSCs (1 × 10⁶) with or without treatment of 7*S*,14*R*-diHDHA were infused into *db/db* mice via tail vein every 5 days for 35 days. Pancreas was collected for histological study. **(A)** Typical images of F4/80+ macrophages (red) in pancreatic cryosections (magnification 200x), and nuclei were counterstained with Hochest 33342; **(B)** quantification of macrophage density in islets (n = 60). The results are mean ± SEM. **p* < 0.05.

3.6. 7S,14R-diHDHA augmented MSC function to increase min6 β-cell viability and insulin secretion

H_2O_2 dose-dependently reduced min6 β-cell viability was measured using the MTT method. When cocultured with MSCs, min6 β-cell viability was significantly increased under H_2O_2 condition (Figure 6A). Additionally, 7*S*,14*R*-diHDHA augmented the MSC effect on increasing min6 β-cell viability (Figure 6A). Furthermore, when min6 β-cells were treated with MSC conditioned medium, min6 β-cells secreted much more insulin (1.3 ± 0.1 vs. 0.9 ± 0.1 ng/mL, *p* < 0.05; Figure 6B), suggesting that MSCs can generate some trophic factors that trigger insulin release. 7*S*,14*R*-diHDHA-treated MSCs further enhanced insulin secretion from Min6 β-cell (1.7 ± 0.1 vs. 1.3 ± 0.1 ng/mL, *p* < 0.05; Figure 6B), which indicates that 7*S*,14*R*-diHDHA can promote MSCs to generate many more trophic factors acting on min6 β-cells to secrete more insulin.
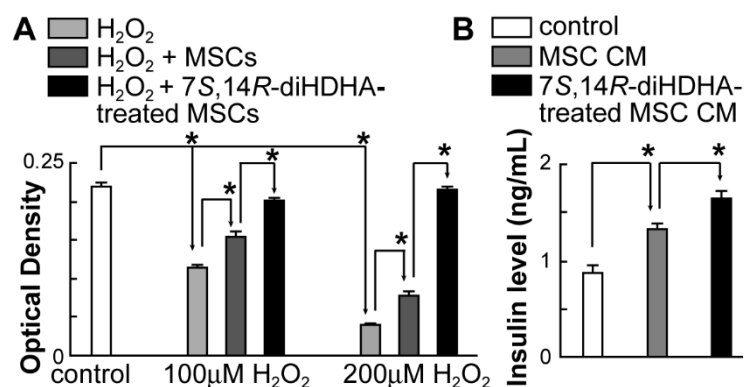
Figure 6. 7*S*,14*R*-diHDHA augmented MSC function to increase min6 β-cell viability and insulin Secretion. **(A)** Min6 β-cells were cocultured with MSCs pretreated with or without 7*S*,14*R*-diHDHA and challenged with 100 or 200 μM H_2O_2. (n = 6). **(B)** Min6 β-cells were treated for 4 h with conditioned medium (CM) of MSCs or 7*S*,14*R*-diHDHA-treated MSCs. Insulin levels were analyzed using ELISA (n = 6). The results are mean ± SEM. * $p < 0.05$.

3.7. 7S,14R-diHDHA treatment enhanced MSC secretion of trophic growth factors

MSCs generate an array of cytokines and growth factors [76,77]. Therefore, we postulated that 7*S*,14*R*-diHDHA treatment enhanced the beneficial effects of MSCs by augmenting their secretion of trophic factors. We observed that 7*S*,14*R*-diHDHA treatment increased the amount of the trophic growth factors VEGF and HGF secreted by MSCs into the cell culture medium (VEGF: 282.5 ± 9.6 vs. 233.0 ± 5.6 pg/mL, $p < 0.05$; 220.7 ± 13.2 vs. 152.3 ± 22.3 pg/mL, $p < 0.05$; Figure 7A, B).
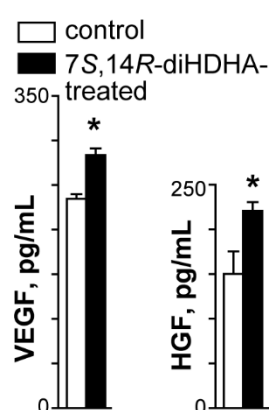

Figure 7. 7*S*,14*R*-diHDHA increased the production of VEGF and HGF by MSCs. MSCs (2 × 10^5) were treated with 7*S*,14*R*-diHDHA (250 nM) for 12 h. The level of VEGF or HGF in the supernatant was analyzed using ELISA kits. VEGF and HGF secretion from MSCs *in vitro* were shown (n = 4). The results are mean ± SEM. *$p < 0.05$ vs. control.

3.8. 7S,14R-diHDHA treatment induced MSC function to decrease pericyte loss in the retina

Vasoregression is the primary pathogenic response of the retina to chronic hyperglycemia. Loss of capillary pericytes, followed by the formation of acellular, nonperfused capillaries, is an attempted compensation for retinal hypoxia [78]. Controlling mellitus can ameliorate diabetic complications; therefore, we want to know whether 7*S*,14*R*-diHDHA-treated MSCs can protect diabetic retinopathy by controlling hyperglycemia. The retinas of *db/db* mice showed a decrease in pericyte density compared with that of the *C57BL/6J* mice (Figure 8). However, MSCs can reduce pericyte loss in *db/db* mice. In addition, 7*S*,14*R*-diHDHA-treated MSCs can further increase the pericyte density compared to untreated MSCs (Figure 8), which suggests that 7*S*,14*R*-diHDHA enhance MSC paracrine function

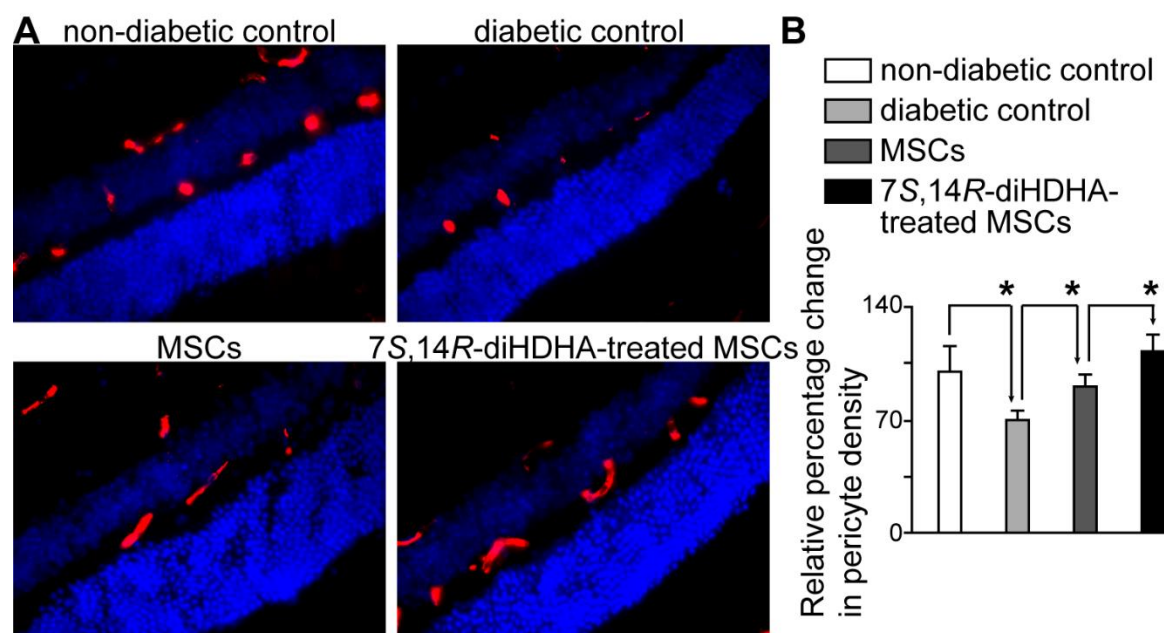to ameliorate retinal pericyte loss in diabetes through adjusting hyperglycemia and acting pericyte directly.

Figure 8. 7*S*,14*R*-diHDHA treatment induced MSC function to decrease pericyte loss in retina. *C57/BL6J* MSCs (1 × 10⁶) with or without treatment of 7*S*,14*R*-diHDHA were infused into *db/db* mice via tail vein every 5 days for 35 days. Eyes were collected for histological study. **(A)** Images of α-SMA⁺ pericytes (red) in retinal sections (magnification 400x), and nuclei were counterstained with Hochest 33342; **(B)** quantification of pericyte density in retina (n = 30). The results are mean ± SEM. * $p < 0.05$.

4. Discussion

Leukocytes produced 7S,14R-diHDHA while P450 and 5-LOX catalyzed the biosynthesis

Taking our current results and previous findings [67] together revealed that leukocytes and their 5-LOX and P450 can produce a novel 7*S*,14*R*-dihydroxy-4*Z*,8*E*,10*Z*,12*E*,16*Z*,19*Z*-DHA or 7*S*,14*R*-diHDHA, a maresin-1 stereoisomer from DHA, as depicted in Figure 1G. We previously found that human P450, including 2D6 (CYP2D6), can catalyze the 14*R*-hydroxylation of DHA, where the contribution of autooxidation is negligible [67]. We observed that human leukocytes can convert 14*R*-HDHA to 7*S*,14*R*-diHDHA. Moreover, we observed that human 5-LOX catalyzed the biosynthesis of 7*S*,14*R*-diHDHA from 14*R*-HDHA by generating 7*S*-hydroxy in 14*R*-HDHA. Therefore, 5-LOX and P450 of leukocytes are accountable for the biogenesis of 7*S*,14*R*-diHDHA since 5-LOX is a major LOX and P450 is readily available in leukocytes [62–64]. The geometries of double-bonds outside of the region from C7 to C14 and the C14 chirality of 14*R*-HDHA are conserved after the transformation to 7,14-diHDHA, based on our results and reported analogous data for eicosanoids [48,79]. Thus, 7*S*,14*R*-diHDHA produced by leukocytes or by sequential catalysis of P450 and 5-LOX is 7*S*,14*R*-dihydroxy-4*Z*,8*E*,10*Z*,12*E*,16*Z*,19*Z*-DHA.

Harnessing mesenchymal stem cells by 7S,14R-diHDHA to ameliorate diabetic mellitus and retinal pericyte loss

The etiologies for type 1 and type 2 diabetes differ. Type 1 diabetes is a chronic autoimmune disease hallmarked by immune-mediated destruction of the pancreatic β-cells. T lymphocytes are aberrantly activated by the antigen-presenting cells in the pancreatic draining lymph nodes, and the activated T lymphocytes then circulate, target, invade the islets and destroyed the β-cells [80,81]. However, type 2 diabetes, hallmarked by underlying insulin resistance, is also characterized by defects in glucose-responsive insulin secretion in addition to an eventual decline in β-cell function

[4,82], and oxidative stress caused by hyperglycemia is considered to be the main reason leading β-cell apoptosis [3,4,6,10,11,83].

MSCs have multiple differentiation and paracrine functions [25]. It has been confirmed that MSC transplantation into STZ-induced type 1 diabetic mouse and NOD models can enhance islet regeneration, lower blood sugar, and increase blood insulin levels [30,32,33,84]. Although MSCs can be recruited to the pancreas, less than 3% of cells migrate to the pancreas [31,85] confirmed the direct differentiation capacity of MSCs is not the main mechanism, which suggests that the paracrine function may confer tissue-repairing function to MSCs. MSCs can generate many bioactive factors, such as TGF-α, HGF, IDO, PGE$_2$, which play important roles in modulating immuno-cell functions, such as inhibiting T cell proliferation, dendritic cell activation, and inflammatory cytokine generation [86,87]. On the basis of generation immunomodulating factors, MSCs inhibit the onset of type 1 diabetes and reverse β-cell functions [23,88]. However, type 2 diabetes is different from type 1 diabetes, and immunomodulating functions may not be the reason for MSCs repairing damaged β-cells in type 2 diabetes. Increased leukocyte infiltration is associated with the onset of type 2 diabetes [89]. Depletion of macrophages by clodronate in liposomes reduced pancreatic invasion of macrophages and destruction of islet β-cells [90,91]. Our results revealed that MSCs can inhibit macrophage infiltration into islets. The increased oxidative stress observed in islets of diabetic states seems to be one of the main factors of deteriorated β-cell function. We have found that MSCs can inhibit macrophage generation of the inflammatory cytokines TNF-α and ROS [57], which indicates the anti-inflammatory functions of MSC protecting β-cell functions in type 2 diabetes.

The islet capillary network is about five times denser than the capillary network of exocrine tissue. The enriched vascularity meets the requirement for the quick secretion of insulin from β-cell in response to blood glucose levels [92]. In diabetic *db/db* mice, the number of endothelial cells was reduced compared with normal nondiabetic mice. VEGF is one of the most important angiogenic cytokines[93]. We have confirmed that MSCs can generate VEGF and promote angiogenesis in wounds, which promotes wound healing in *db/db* mice [54]. MSCs promote vascularity in islets of *db/db* mice may also through generating VEGF.

DHA is a typical ω-3 long-chain poly-unsaturated fatty acid, it can be transformed enzymatically into potent inflammation-resolving lipid mediators, such as Resolvin D series [41], neuroprotectin/protectins [46–49], maresins [58,59], maresin-likes [67], and 7*S*,14*R*-diHDHA. We also found a DHA-derived lipid mediators 14*S*,21*R*-diHDHA, which can enhance MSC functions to promote wound healing and repair acute kidney injury [54,57]. 7*S*,14*R*-diHDHA is a new lipid mediator that has a potential anti-inflammatory function. In this study, we observed that 7*S*,14*R*-diHDHA can promote MSC paracrine function to generate VEGF and HGF. HGF has anti-inflammatory properties; it can increase IL-10 levels and reduce IL-1β levels in pancreatitis or diabetes [94–96]. These data suggest that 7*S*,14*R*-diHDHA promotes MSC functions to ameliorate diabetic mellitus mainly by enhancing MSC paracrine functions. These results are consistent with reports that maresins promote the beneficial bioactions of stem cells in the treatment of diseases [59]. Maresin 1 regulates insulin signaling in human adipocytes as well as in adipose tissue and muscle of lean and obese mice [59]. Maresin 1 inhibits hyperglycemia-induced ferroptosis [60].

Diabetic retinopathy is a clinically well-defined, sight-threatening, chronic microvascular complication that eventually affects virtually all patients with diabetes. Diabetic retinopathy is characterized by gradually progressive alterations in the retinal microvasculature, which start with the loss of the two cellular components of retinal capillaries: the pericyte, a vessel support cell, and the endothelial cell, and pericytes disappear before endothelial cells start to vanish [39,40,97]. *db/db* mice develop hyperglycemia starting at 8-week age as a result of excessive food consumption [98,99]. They show early signs of diabetic retinopathy, such as thickening of capillary basement membrane at 22 weeks [100] and loss of pericytes in retinas at 26 weeks, followed by endothelial cell loss at 34 weeks [101]. In our study, pericyte loss occurred as early as 22 weeks of age in *db/db* mice. MSCs can inhibit pericyte loss. Moreover, 7*S*,14*R*-diHDHA-treated MSCs further markedly increased pericyte density compared with untreated MSCs. This suggests that 7*S*,14*R*-diHDHA enhances MSC paracrine function to ameliorate retinal pericyte loss in diabetes by adjusting for hyperglycemia

and/or acting pericyte directly. This enhancement is likely to occur through MSC secretion of VEGF, as 7*S*,14*R*-diHDHA can significantly promote MSC production of VEGF (Figure 7), and VEGF is thought to be an important cytokine inducing vasoregeneration in diabetic retinopathy [78]. When MSCs were infused into diabetic mice, MSCs have an anti-inflammatory function, reducing oxidative stress. Under this condition, VEGF or HGF generated from MSCs may trigger the PI3K/AKT signaling pathway and maintain retinal vascular integrity [102,103], while 7*S*,14*R*-diHDHA treatment can enhance MSC function via this pathway. The mechanism for the amelioration of diabetic damage of retinal pericytes by 7*S*,14*R*-diHDHA-treated MSCs is also likely attributable to their amelioration of diabetes, especially diabetic hyperglycemia.

Future directions

The scope of this pilot study provides multiple opportunities for future research. 5-LOX could convert DHA to 7*S*-hydroxyl DHA first, followed by P450 14*R*-hydroxylation in sequential enzymatic catalysis to generate 7*S*,14*R*-diHDHA from DHA. However, the exact P450 enzymes involved in 14*R*-hydroxylation are unknown. The appearance of 7*S*,14*R*-diHDHA in the blood, pancreas, and other organs *in vivo* in animals and humans under healthy and diabetic conditions is likely to be transient, which needs to be studied systematically at different time points. We will study the actions of 7*S*,14*R*-diHDHA alone. Future studies should also evaluate the effect of our treatments on the other aspects of diabetes and on diabetic retinopathy.

5. Conclusions

We identified a novel DHA-derived 7*S*,14*R*-dihydroxy-4*Z*,8*E*,10*Z*,*12E*,16*Z*,19*Z*-DHA (7*S*,14*R*-diHDHA), a maresin-1 stereoisomer, biosynthesized by leukocytes and related P450 and 5-LOX enzymes [62–64]. 7*S*,14*R*-diHDHA promoted MSC paracrine functions in *db/db* mice *in vivo* to ameliorate diabetic mellitus through improving β-cell function, lowering blood sugar, improving glucose tolerance, and increasing blood insulin levels. It augmented the proportion of β-cells and reduced that of α-cells to total islet pancreatic cells, and decreased the number of macrophages in islets in *db/db* mice *in vivo*. Also, the lipid mediator enhanced MSC function to increase min6 β-cell viability and insulin and MSC secretion of trophic growth factors. Furthermore, 7*S*,14*R*-diHDHA treatment induced MSC function to decrease pericyte loss in the retinas of diabetic *db/db* mice *in vivo*. Taken together, pretreatment of MSCs with 14*S*,21*R*-diHDHA or related LMs or structural mimics may offer a new clinical strategy for improved treatment of diabetic mellitus and diabetic complications.

Institutional Review Board Statement: The Institutional Review Board protocol was authorized and approved by the Institutional Review Board of Louisiana State University, Health, New Orleans, USA. The animal use protocol was authorized and approved by the Institutional Animal Care and Use Committee of Louisiana State University, Health, New Orleans, USA.

Data Availability Statement: Data is contained within the article.

Conflicts of Interest: The authors do not have any conflict of interest.

References

1.   Florez, J.C. Newly identified loci highlight beta cell dysfunction as a key cause of type 2 diabetes: where are the insulin resistance genes? *Diabetologia* **2008**, *51*, 1100-1110.

2. Gunton, J.E.; Kulkarni, R.N.; Yim, S.; Okada, T.; Hawthorne, W.J.; Tseng, Y.H.; Roberson, R.S.; Ricordi, C.; O'Connell, P.J.; Gonzalez, F.J.; et al. Loss of ARNT/HIF1beta mediates altered gene expression and pancreatic-islet dysfunction in human type 2 diabetes. *Cell* **2005**, *122*, 337-349.

3. Cerf, M.E. Beta cell dysfunction and insulin resistance. *Frontiers in endocrinology* **2013**, *4*, 37. https://doi.org/10.3389/fendo.2013.00037.

4. Dludla, P.V.; Mabhida, S.E.; Ziqubu, K.; Nkambule, B.B.; Mazibuko-Mbeje, S.E.; Hanser, S.; Basson, A.K.; Pheiffer, C.; Kengne, A.P. Pancreatic beta-cell dysfunction in type 2 diabetes: Implications of inflammation and oxidative stress. *World journal of diabetes* **2023**, *14*, 130-146. https://doi.org/10.4239/wjd.v14.i3.130.

5. Tiedge, M.; Lortz, S.; Drinkgern, J.; Lenzen, S. Relation between antioxidant enzyme gene expression and antioxidative defense status of insulin-producing cells. *Diabetes* **1997**, *46*, 1733-1742.

6. Eguchi, N.; Vaziri, N.D.; Dafoe, D.C.; Ichii, H. The Role of Oxidative Stress in Pancreatic beta Cell Dysfunction in Diabetes. *International journal of molecular sciences* **2021**, *22*. https://doi.org/10.3390/ijms22041509.

7. Butler, A.E.; Janson, J.; Bonner-Weir, S.; Ritzel, R.; Rizza, R.A.; Butler, P.C. Beta-cell deficit and increased beta-cell apoptosis in humans with type 2 diabetes. *Diabetes* **2003**, *52*, 102-110.

8. Pick, A.; Clark, J.; Kubstrup, C.; Levisetti, M.; Pugh, W.; Bonner-Weir, S.; Polonsky, K.S. Role of apoptosis in failure of beta-cell mass compensation for insulin resistance and beta-cell defects in the male Zucker diabetic fatty rat. *Diabetes* **1998**, *47*, 358-364.

9. Puff, R.; Dames, P.; Weise, M.; Goke, B.; Seissler, J.; Parhofer, K.G.; Lechner, A. Reduced proliferation and a high apoptotic frequency of pancreatic beta cells contribute to genetically-determined diabetes susceptibility of db/db BKS mice. *Horm Metab Res* **2011**, *43*, 306-311.

10. Inaishi, J.; Saisho, Y. Beta-Cell Mass in Obesity and Type 2 Diabetes, and Its Relation to Pancreas Fat: A Mini-Review. *Nutrients* **2020**, *12*. https://doi.org/10.3390/nu12123846.

11. Miranda, M.A.; Carson, C.; St Pierre, C.L.; Macias-Velasco, J.F.; Hughes, J.W.; Kunzmann, M.; Schmidt, H.; Wayhart, J.P.; Lawson, H.A. Spontaneous restoration of functional beta-cell mass in obese SM/J mice. *Physiological reports* **2020**, *8*, e14573. https://doi.org/10.14814/phy2.14573.

12. Intensive blood-glucose control with sulphonylureas or insulin compared with conventional treatment and risk of complications in patients with type 2 diabetes (UKPDS 33). UK Prospective Diabetes Study (UKPDS) Group. *Lancet* **1998**, *352*, 837-853.

13. Want, L.L. Optimizing treatment success with an amylin analogue. *Diabetes Educ* **2008**, *34 Suppl 1*, 11S-17S.

14. Group, G.S.R.; Nathan, D.M.; Lachin, J.M.; Balasubramanyam, A.; Burch, H.B.; Buse, J.B.; Butera, N.M.; Cohen, R.M.; Crandall, J.P.; Kahn, S.E.; et al. Glycemia Reduction in Type 2 Diabetes - Glycemic Outcomes. *The New England journal of medicine* **2022**, *387*, 1063-1074. https://doi.org/10.1056/NEJMoa2200433.

15. Efanova, I.B.; Zaitsev, S.V.; Zhivotovsky, B.; Kohler, M.; Efendic, S.; Orrenius, S.; Berggren, P.O. Glucose and tolbutamide induce apoptosis in pancreatic beta-cells. A process dependent on intracellular Ca2+ concentration. *The Journal of biological chemistry* **1998**, *273*, 33501-33507.

16. Hakobyan, L.; Haaijer-Ruskamp, F.M.; de Zeeuw, D.; Dobre, D.; Denig, P. Comparing adverse event rates of oral blood glucose-lowering drugs reported by patients and healthcare providers: a post-hoc analysis of observational studies published between 1999 and 2011. *Drug Saf* **2011**, *34*, 1191-1202.

17. Dalle, S.; Abderrahmani, A.; Renard, E. Pharmacological inhibitors of beta-cell dysfunction and death as therapeutics for diabetes. *Frontiers in endocrinology* **2023**, *14*, 1076343. https://doi.org/10.3389/fendo.2023.1076343.

18. Shao, J.; Iwashita, N.; Ikeda, F.; Ogihara, T.; Uchida, T.; Shimizu, T.; Uchino, H.; Hirose, T.; Kawamori, R.; Watada, H. Beneficial effects of candesartan, an angiotensin II type 1 receptor blocker, on beta-cell function and morphology in db/db mice. *Biochem Biophys Res Commun* **2006**, *344*, 1224-1233.

19. Lee, J.W.; Gu, H.O.; Jung, Y.; Jung, Y.; Seo, S.Y.; Hong, J.H.; Hong, I.S.; Lee, D.H.; Kim, O.H.; Oh, B.C. Candesartan, an angiotensin-II receptor blocker, ameliorates insulin resistance and hepatosteatosis by reducing intracellular calcium overload and lipid accumulation. *Experimental & molecular medicine* **2023**, *55*, 910-925. https://doi.org/10.1038/s12276-023-00982-6.

20. Chen, H.; Zhou, W.; Ruan, Y.; Yang, L.; Xu, N.; Chen, R.; Yang, R.; Sun, J.; Zhang, Z. Reversal of angiotensin ll-induced beta-cell dedifferentiation via inhibition of NF-kappab signaling. *Molecular medicine* **2018**, *24*, 43. https://doi.org/10.1186/s10020-018-0044-3.

21. Harmon, J.S.; Bogdani, M.; Parazzoli, S.D.; Mak, S.S.; Oseid, E.A.; Berghmans, M.; Leboeuf, R.C.; Robertson, R.P. beta-Cell-specific overexpression of glutathione peroxidase preserves intranuclear MafA and reverses diabetes in db/db mice. *Endocrinology* **2009**, *150*, 4855-4862.

22. Robertson, R.P. Nrf2 and Antioxidant Response in Animal Models of Type 2 Diabetes. *International journal of molecular sciences* **2023**, *24*. https://doi.org/10.3390/ijms24043082.

23. Vija, L.; Farge, D.; Gautier, J.F.; Vexiau, P.; Dumitrache, C.; Bourgarit, A.; Verrecchia, F.; Larghero, J. Mesenchymal stem cells: Stem cell therapy perspectives for type 1 diabetes. *Diabetes Metab* **2009**, *35*, 85-93.

24. Bernardi, S.; Severini, G.M.; Zauli, G.; Secchiero, P. Cell-based therapies for diabetic complications. *Exp Diabetes Res* **2012**, *2012*, 872504.

25. Miklosz, A.; Chabowski, A. Adipose-derived Mesenchymal Stem Cells Therapy as a new Treatment Option for Diabetes Mellitus. *The Journal of clinical endocrinology and metabolism* **2023**, *108*, 1889-1897. https://doi.org/10.1210/clinem/dgad142.

26. Aglan, H.A.; Kotob, S.E.; Mahmoud, N.S.; Kishta, M.S.; Ahmed, H.H. Bone marrow stem cell-derived beta-cells: New issue for diabetes cell therapy. *Tissue & cell* **2024**, *86*, 102280. https://doi.org/10.1016/j.tice.2023.102280.

27. Hess, D.; Li, L.; Martin, M.; Sakano, S.; Hill, D.; Strutt, B.; Thyssen, S.; Gray, D.A.; Bhatia, M. Bone marrow-derived stem cells initiate pancreatic regeneration. *Nat Biotechnol* **2003**, *21*, 763-770.

28. Zhoujun, Z.; Bingzheng, F.; Yuwei, Y.; Yingying, Z.; Zhiran, X.; Chunhua, H.; Jing, L.; Haibo, T.; Wanli, L.; Ting, Z.; et al. Transplantation of insulin-producing cells derived from human MSCs to treat diabetes in a non-human primate model. *Artificial organs* **2023**, *47*, 1298-1308. https://doi.org/10.1111/aor.14538.

29. Boumaza, I.; Srinivasan, S.; Witt, W.T.; Feghali-Bostwick, C.; Dai, Y.; Garcia-Ocana, A.; Feili-Hariri, M. Autologous bone marrow-derived rat mesenchymal stem cells promote PDX-1 and insulin expression in the islets, alter T cell cytokine pattern and preserve regulatory T cells in the periphery and induce sustained normoglycemia. *J Autoimmun* **2009**, *32*, 33-42.

30. Yousef, H.N.; Sakr, S.M.; Sabry, S.A. Mesenchymal Stem Cells Ameliorate Hyperglycemia in Type I Diabetic Developing Male Rats. *Stem cells international* **2022**, *2022*, 7556278. https://doi.org/10.1155/2022/7556278.

31. Lee, R.H.; Seo, M.J.; Reger, R.L.; Spees, J.L.; Pulin, A.A.; Olson, S.D.; Prockop, D.J. Multipotent stromal cells from human marrow home to and promote repair of pancreatic islets and renal glomeruli in diabetic NOD/scid mice. *Proc Natl Acad Sci U S A* **2006**, *103*, 17438-17443.

32. Gabr, M.M.; Zakaria, M.M.; Refaie, A.F.; Ismail, A.M.; Abou-El-Mahasen, M.A.; Ashamallah, S.A.; Khater, S.M.; El-Halawani, S.M.; Ibrahim, R.Y.; Uin, G.S.; et al. Insulin-producing cells from adult human bone marrow mesenchymal stem cells control streptozotocin-induced diabetes in nude mice. *Cell transplantation* **2013**, *22*, 133-145. https://doi.org/10.3727/096368912X647162.

33. Carlsson, P.O.; Espes, D.; Sisay, S.; Davies, L.C.; Smith, C.I.E.; Svahn, M.G. Umbilical cord-derived mesenchymal stromal cells preserve endogenous insulin production in type 1 diabetes: a Phase I/II randomised double-blind placebo-controlled trial. *Diabetologia* **2023**, *66*, 1431-1441. https://doi.org/10.1007/s00125-023-05934-3.

34. Wang, L.; Zhao, S.; Mao, H.; Zhou, L.; Wang, Z.J.; Wang, H.X. Autologous bone marrow stem cell transplantation for the treatment of type 2 diabetes mellitus. *Chin Med J (Engl)* **2011**, *124*, 3622-3628.

35. Mathur, A.; Taurin, S.; Alshammary, S. The Safety and Efficacy of Mesenchymal Stem Cells in the Treatment of Type 2 Diabetes- A Literature Review. *Diabetes, metabolic syndrome and obesity : targets and therapy* **2023**, *16*, 769-777. https://doi.org/10.2147/DMSO.S392161.

36. Kornicka, K.; Houston, J.; Marycz, K. Dysfunction of Mesenchymal Stem Cells Isolated from Metabolic Syndrome and Type 2 Diabetic Patients as Result of Oxidative Stress and Autophagy may Limit Their Potential Therapeutic Use. *Stem cell reviews and reports* **2018**, *14*, 337-345. https://doi.org/10.1007/s12015-018-9809-x.

37. Yin, M.; Zhang, Y.; Yu, H.; Li, X. Role of Hyperglycemia in the Senescence of Mesenchymal Stem Cells. *Frontiers in cell and developmental biology* **2021**, *9*, 665412. https://doi.org/10.3389/fcell.2021.665412.

38. Bhavsar, A.R. Diabetic retinopathy: the latest in current management. *Retina* **2006**, *26*, S71-79.

39. Gange, W.S.; Lopez, J.; Xu, B.Y.; Lung, K.; Seabury, S.A.; Toy, B.C. Incidence of Proliferative Diabetic Retinopathy and Other Neovascular Sequelae at 5 Years Following Diagnosis of Type 2 Diabetes. *Diabetes care* **2021**, *44*, 2518-2526. https://doi.org/10.2337/dc21-0228.

40. Eshaq, R.S.; Aldalati, A.M.Z.; Alexander, J.S.; Harris, N.R. Diabetic retinopathy: Breaking the barrier. *Pathophysiology : the official journal of the International Society for Pathophysiology* **2017**, *24*, 229-241. https://doi.org/10.1016/j.pathophys.2017.07.001.

41. Spite, M.; Serhan, C.N. Novel lipid mediators promote resolution of acute inflammation: impact of aspirin and statins. *Circ Res* **2010**, *107*, 1170-1184.

42. Marcheselli, V.L.; Hong, S.; Lukiw, W.J.; Tian, X.H.; Gronert, K.; Musto, A.; Hardy, M.; Gimenez, J.M.; Chiang, N.; Serhan, C.N.; et al. Novel docosanoids inhibit brain ischemia-reperfusion-mediated leukocyte infiltration and pro-inflammatory gene expression. *The Journal of biological chemistry* **2003**, *278*, 43807-43817.

43. Antony, R.; Lukiw, W.J.; Bazan, N.G. Neuroprotectin D1 induces dephosphorylation of Bcl-xL in a PP2A-dependent manner during oxidative stress and promotes retinal pigment epithelial cell survival. *The Journal of biological chemistry* **2010**, *285*, 18301-18308.

44. Pham, T.L.; Bazan, H.E.P. Docosanoid signaling modulates corneal nerve regeneration: effect on tear secretion, wound healing, and neuropathic pain. *Journal of lipid research* **2021**, *62*, 100033. https://doi.org/10.1194/jlr.TR120000954.

45. Cortina, M.S.; He, J.; Russ, T.; Bazan, N.G.; Bazan, H.E. Neuroprotectin D1 restores corneal nerve integrity and function after damage from experimental surgery. *Investigative ophthalmology & visual science* **2013**, *54*, 4109-4116.

46. Mukherjee, P.K.; Marcheselli, V.L.; Serhan, C.N.; Bazan, N.G. Neuroprotectin D1: a docosahexaenoic acid-derived docosatriene protects human retinal pigment epithelial cells from oxidative stress. *Proc Natl Acad Sci U S A* **2004**, *101*, 8491-8496.

47. Zhao, Y.; Calon, F.; Julien, C.; Winkler, J.W.; Petasis, N.A.; Lukiw, W.J.; Bazan, N.G. Docosahexaenoic acid-derived neuroprotectin D1 induces neuronal survival via secretase- and PPARgamma-mediated mechanisms in Alzheimer's disease models. *PloS one* **2011**, *6*, e15816.

48. Hong, S.; Gronert, K.; Devchand, P.R.; Moussignac, R.L.; Serhan, C.N. Novel docosatrienes and 17S-resolvins generated from docosahexaenoic acid in murine brain, human blood, and glial cells. Autacoids in anti-inflammation. *The Journal of biological chemistry* **2003**, *278*, 14677-14687.

49. Hong, S.; Tian, H.; Lu, Y.; Laborde, J.M.; Muhale, F.A.; Wang, Q.; Alapure, B.V.; Serhan, C.N.; Bazan, N.G. Neuroprotectin/protectin D1: endogenous biosynthesis and actions on diabetic macrophages in promoting wound healing and innervation impaired by diabetes. *American journal of physiology. Cell physiology* **2014**, *307*, C1058-1067.

50. Emre, C.; Arroyo-Garcia, L.E.; Do, K.V.; Jun, B.; Ohshima, M.; Alcalde, S.G.; Cothern, M.L.; Maioli, S.; Nilsson, P.; Hjorth, E.; et al. Intranasal delivery of pro-resolving lipid mediators rescues memory and gamma oscillation impairment in App(NL-G-F/NL-G-F) mice. *Communications biology* **2022**, *5*, 245. https://doi.org/10.1038/s42003-022-03169-3.

51. Emre, C.; Do, K.V.; Jun, B.; Hjorth, E.; Alcalde, S.G.; Kautzmann, M.I.; Gordon, W.C.; Nilsson, P.; Bazan, N.G.; Schultzberg, M. Age-related changes in brain phospholipids and bioactive lipids in the APP knock-in mouse model of Alzheimer's disease. *Acta neuropathologica communications* **2021**, *9*, 116. https://doi.org/10.1186/s40478-021-01216-4.

52. Asatryan, A.; Bazan, N.G. Molecular mechanisms of signaling via the docosanoid neuroprotectin D1 for cellular homeostasis and neuroprotection. *The Journal of biological chemistry* **2017**, *292*, 12390-12397. https://doi.org/10.1074/jbc.R117.783076.

53. Pham, T.L.; He, J.; Kakazu, A.H.; Jun, B.; Bazan, N.G.; Bazan, H.E.P. Defining a mechanistic link between pigment epithelium-derived factor, docosahexaenoic acid, and corneal nerve regeneration. *The Journal of biological chemistry* **2017**, *292*, 18486-18499. https://doi.org/10.1074/jbc.M117.801472.

54. Tian, H.; Lu, Y.; Shah, S.P.; Hong, S. 14S,21R-Dihydroxydocosahexaenoic Acid Remedies Impaired Healing and Mesenchymal Stem Cell Functions in Diabetic Wounds. *The Journal of biological chemistry* **2011**, *286*, 4443-4453.

55. Lu, Y.; Tian, H.; Hong, S. Novel 14,21-dihydroxy-docosahexaenoic acids: structures, formation pathways, and enhancement of wound healing. *Journal of lipid research* **2010**, *51*, 923-932.

56. Bazan, N.G. Cell survival matters: docosahexaenoic acid signaling, neuroprotection and photoreceptors. *Trends in neurosciences* **2006**, *29*, 263-271. https://doi.org/10.1016/j.tins.2006.03.005.

57. Tian, H.; Lu, Y.; Shah, S.P.; Wang, Q.; Hong, S. 14S,21R-dihydroxy-docosahexaenoic acid treatment enhances mesenchymal stem cell amelioration of renal ischemia/reperfusion injury. *Stem Cells Dev* **2012**, *21*, 1187-1199. https://doi.org/10.1089/scd.2011.0220.

58. Serhan, C.N.; Yang, R.; Martinod, K.; Kasuga, K.; Pillai, P.S.; Porter, T.F.; Oh, S.F.; Spite, M. Maresins: novel macrophage mediators with potent antiinflammatory and proresolving actions. *J Exp Med* **2009**, *206*, 15-23.

59. Martinez-Fernandez, L.; Gonzalez-Muniesa, P.; Sainz, N.; Escote, X.; Martinez, J.A.; Arbones-Mainar, J.M.; Moreno-Aliaga, M.J. Maresin 1 regulates insulin signaling in human adipocytes as well as in adipose tissue and muscle of lean and obese mice. *Journal of physiology and biochemistry* **2021**, *77*, 167-173. https://doi.org/10.1007/s13105-020-00775-9.

60. Li, Y.; Liu, J.; Ma, X.; Bai, X. Maresin-1 inhibits high glucose induced ferroptosis in ARPE-19 cells by activating the Nrf2/HO-1/GPX4 pathway. *BMC ophthalmology* **2023**, *23*, 368. https://doi.org/10.1186/s12886-023-03115-9.

61. Shindou, H.; Koso, H.; Sasaki, J.; Nakanishi, H.; Sagara, H.; Nakagawa, K.M.; Takahashi, Y.; Hishikawa, D.; Iizuka-Hishikawa, Y.; Tokumasu, F.; et al. Docosahexaenoic acid preserves visual function by maintaining correct disc morphology in retinal photoreceptor cells. *The Journal of biological chemistry* **2017**, *292*, 12054-12064. https://doi.org/10.1074/jbc.M117.790568.

62. el Makhour-Hojeij, Y.; Baclet, M.C.; Chable-Rabinovitch, H.; Beneytout, J.L.; Cook, J. Expression of 5-lipoxygenase in lymphoblastoid B and T cells. *Prostaglandins* **1994**, *48*, 21-29. https://doi.org/10.1016/0090-6980(94)90093-0.

63. Cook-Moreau, J.M.; El-Makhour Hojeij, Y.; Barriere, G.; Rabinovitch-Chable, H.C.; Faucher, K.S.; Sturtz, F.G.; Rigaud, M.A. Expression of 5-lipoxygenase (5-LOX) in T lymphocytes. *Immunology* **2007**, *122*, 157-166. https://doi.org/10.1111/j.1365-2567.2007.02621.x.

64. Radmark, O.; Samuelsson, B. 5-Lipoxygenase: mechanisms of regulation. *Journal of lipid research* **2009**, *50 Suppl*, S40-45. https://doi.org/10.1194/jlr.R800062-JLR200.

65. Izadpanah, R.; Trygg, C.; Patel, B.; Kriedt, C.; Dufour, J.; Gimble, J.M.; Bunnell, B.A. Biologic properties of mesenchymal stem cells derived from bone marrow and adipose tissue. *J Cell Biochem* **2006**, *99*, 1285-1297.

66. Serhan, C.N.; Romano, M. Lipoxin biosynthesis and actions: role of the human platelet LX-synthase. *J Lipid Mediat Cell Signal* **1995**, *12*, 293-306.

67. Hong, S.; Lu, Y.; Tian, H.; Alapure, B.V.; Wang, Q.; Bunnell, B.A.; Laborde, J.M. Maresin-like lipid mediators are produced by leukocytes and platelets and rescue reparative function of diabetes-impaired macrophages. *Chem Biol* **2014**, *21*, 1318-1329. https://doi.org/10.1016/j.chembiol.2014.06.010.

68. Cheng, Y.; Wang, Y.; Wang, X.; Jiang, Z.; Zhu, L.; Fang, S. Neutrophil-to-Lymphocyte Ratio, Platelet-to-Lymphocyte Ratio, and Monocyte-to-Lymphocyte Ratio in Depression: An Updated Systematic Review and Meta-Analysis. *Frontiers in psychiatry* **2022**, *13*, 893097. https://doi.org/10.3389/fpsyt.2022.893097.

69. Lee, J.S.; Kim, N.Y.; Na, S.H.; Youn, Y.H.; Shin, C.S. Reference values of neutrophil-lymphocyte ratio, lymphocyte-monocyte ratio, platelet-lymphocyte ratio, and mean platelet volume in healthy adults in South Korea. *Medicine* **2018**, *97*, e11138. https://doi.org/10.1097/MD.0000000000011138.

70. Baravkar, S.B.; Lu, L.; Masoud, A.R.; Zhao, Q.; He, J.; Hong, S. Development of a Novel Covalently Bonded Conjugate of Caprylic Acid Tripeptide (Isoleucine–Leucine–Aspartic Acid) for Wound-Compatible and Injectable Hydrogel to Accelerate Healing. *biomolecules* **2024**, *14*, 94.

71. Percie du Sert, N.; Hurst, V.; Ahluwalia, A.; Alam, S.; Avey, M.T.; Baker, M.; Browne, W.J.; Clark, A.; Cuthill, I.C.; Dirnagl, U.; et al. The ARRIVE guidelines 2.0: Updated guidelines for reporting animal research. *J Cereb Blood Flow Metab* **2020**, *40*, 1769-1777. https://doi.org/10.1177/0271678X20943823.

72. Hellmann, J.; Tang, Y.; Spite, M. Proresolving lipid mediators and diabetic wound healing. *Curr Opin Endocrinol Diabetes Obes* **2012**, *19*, 104-108. https://doi.org/10.1097/MED.0b013e3283514e00.

73. Tian, H.; Lu, Y.; Shah, S.P.; Hong, S. Autacoid 14S,21R-dihydroxy-docosahexaenoic acid counteracts diabetic impairment of macrophage prohealing functions. *Am J Pathol* **2011**, *179*, 1780-1791. https://doi.org/10.1016/j.ajpath.2011.06.026.

74. Schneider, C.; Yu, Z.; Boeglin, W.E.; Zheng, Y.; Brash, A.R. Enantiomeric separation of hydroxy and hydroperoxy eicosanoids by chiral column chromatography. *Methods Enzymol* **2007**, *433*, 145-157.

75. Yin, H.; Gao, L.; Tai, H.H.; Murphey, L.J.; Porter, N.A.; Morrow, J.D. Urinary prostaglandin F2alpha is generated from the isoprostane pathway and not the cyclooxygenase in humans. *The Journal of biological chemistry* **2007**, *282*, 329-336.

76. Wu, Y.; Chen, L.; Scott, P.G.; Tredget, E.E. Mesenchymal stem cells enhance wound healing through differentiation and angiogenesis. *Stem Cells* **2007**, *25*, 2648-2659.

77. Shi, Y.; Su, J.; Roberts, A.I.; Shou, P.; Rabson, A.B.; Ren, G. How mesenchymal stem cells interact with tissue immune responses. *Trends Immunol* **2012**, *33*, 136-143.

78. Hammes, H.P.; Feng, Y.; Pfister, F.; Brownlee, M. Diabetic retinopathy: targeting vasoregression. *Diabetes* **2011**, *60*, 9-16.

79. Capdevila, J.H.; Holla, V.R.; Faick, J.R. Cytochrome P450 and the Metabolism and Bioactivation of Arachidonic Acid and Eicosanoids. In *Cytochrome P450: Structure, Mechanism, and Biochemistry, 3e*, Paul, R.O.d.M., Ed.; Kluwer Academic/Plenum Publishers: New York, 2005.

80. Mathis, D.; Vence, L.; Benoist, C. beta-Cell death during progression to diabetes. *Nature* **2001**, *414*, 792-798.

81. Pugliese, A. Autoreactive T cells in type 1 diabetes. *The Journal of clinical investigation* **2017**, *127*, 2881-2891. https://doi.org/10.1172/JCI94549.

82. Rhodes, C.J. Type 2 diabetes-a matter of beta-cell life and death? *Science* **2005**, *307*, 380-384.

83. Dinic, S.; Arambasic Jovanovic, J.; Uskokovic, A.; Mihailovic, M.; Grdovic, N.; Tolic, A.; Rajic, J.; Dordevic, M.; Vidakovic, M. Oxidative stress-mediated beta cell death and dysfunction as a target for diabetes management. *Frontiers in endocrinology* **2022**, *13*, 1006376. https://doi.org/10.3389/fendo.2022.1006376.

84. Jurewicz, M.; Yang, S.; Augello, A.; Godwin, J.G.; Moore, R.F.; Azzi, J.; Fiorina, P.; Atkinson, M.; Sayegh, M.H.; Abdi, R. Congenic mesenchymal stem cell therapy reverses hyperglycemia in experimental type 1 diabetes. *Diabetes* **2010**, *59*, 3139-3147.

85. Preda, M.B.; Neculachi, C.A.; Fenyo, I.M.; Vacaru, A.M.; Publik, M.A.; Simionescu, M.; Burlacu, A. Short lifespan of syngeneic transplanted MSC is a consequence of in vivo apoptosis and immune cell recruitment in mice. *Cell death & disease* **2021**, *12*, 566. https://doi.org/10.1038/s41419-021-03839-w.

86. Soleymaninejadian, E.; Pramanik, K.; Samadian, E. Immunomodulatory properties of mesenchymal stem cells: cytokines and factors. *Am J Reprod Immunol* **2012**, *67*, 1-8.

87. Jiang, W.; Xu, J. Immune modulation by mesenchymal stem cells. *Cell proliferation* **2020**, *53*, e12712. https://doi.org/10.1111/cpr.12712.

88. Jayasinghe, M.; Prathiraja, O.; Perera, P.B.; Jena, R.; Silva, M.S.; Weerawarna, P.S.H.; Singhal, M.; Kayani, A.M.A.; Karnakoti, S.; Jain, S. The Role of Mesenchymal Stem Cells in the Treatment of Type 1 Diabetes. *Cureus* **2022**, *14*, e27337. https://doi.org/10.7759/cureus.27337.

89. Ford, E.S. Leukocyte count, erythrocyte sedimentation rate, and diabetes incidence in a national sample of US adults. *Am J Epidemiol* **2002**, *155*, 57-64.

90. Inokuchi, C.; Ueda, H.; Hamaguchi, T.; Miyagawa, J.; Shinohara, M.; Okamura, H.; Namba, M. Role of macrophages in the development of pancreatic islet injury in spontaneously diabetic torii rats. *Exp Anim* **2009**, *58*, 383-394.

91. Chan, J.Y.; Lee, K.; Maxwell, E.L.; Liang, C.; Laybutt, D.R. Macrophage alterations in islets of obese mice linked to beta cell disruption in diabetes. *Diabetologia* **2019**, *62*, 993-999. https://doi.org/10.1007/s00125-019-4844-y.

92. Konstantinova, I.; Lammert, E. Microvascular development: learning from pancreatic islets. *Bioessays* **2004**, *26*, 1069-1075.

93. Li, J.; Zhang, Y.P.; Kirsner, R.S. Angiogenesis in wound repair: angiogenic growth factors and the extracellular matrix. *Microsc Res Tech* **2003**, *60*, 107-114.

94. Warzecha, Z.; Dembinski, A.; Ceranowicz, P.; Konturek, S.; Tomaszewska, R.; Stachura, J.; Nakamura, T.; Konturek, P.C. Inhibition of cyclooxygenase-2 reduces the protective effect of hepatocyte growth factor in experimental pancreatitis. *Eur J Pharmacol* **2004**, *486*, 107-119.

95. Greer, P.J.; Lee, P.J.; Paragomi, P.; Stello, K.; Phillips, A.; Hart, P.; Speake, C.; Lacy-Hulbert, A.; Whitcomb, D.C.; Papachristou, G.I. Severe acute pancreatitis exhibits distinct cytokine signatures and trajectories in humans: a prospective observational study. *American journal of physiology. Gastrointestinal and liver physiology* **2022**, *323*, G428-G438. https://doi.org/10.1152/ajpgi.00100.2022.

96. Oliveira, A.G.; Araujo, T.G.; Carvalho, B.M.; Rocha, G.Z.; Santos, A.; Saad, M.J.A. The Role of Hepatocyte Growth Factor (HGF) in Insulin Resistance and Diabetes. *Frontiers in endocrinology* **2018**, *9*, 503. https://doi.org/10.3389/fendo.2018.00503.

97. Hammes, H.P.; Lin, J.; Wagner, P.; Feng, Y.; Vom Hagen, F.; Krzizok, T.; Renner, O.; Breier, G.; Brownlee, M.; Deutsch, U. Angiopoietin-2 causes pericyte dropout in the normal retina: evidence for involvement in diabetic retinopathy. *Diabetes* **2004**, *53*, 1104-1110.

98. Kodama, H.; Fujita, M.; Yamaguchi, I. Development of hyperglycaemia and insulin resistance in conscious genetically diabetic (C57BL/KsJ-db/db) mice. *Diabetologia* **1994**, *37*, 739-744.

99. Dalboge, L.S.; Almholt, D.L.; Neerup, T.S.; Vassiliadis, E.; Vrang, N.; Pedersen, L.; Fosgerau, K.; Jelsing, J. Characterisation of age-dependent beta cell dynamics in the male db/db mice. *PloS one* **2013**, *8*, e82813. https://doi.org/10.1371/journal.pone.0082813.

100. Clements, R.S., Jr.; Robison, W.G., Jr.; Cohen, M.P. Anti-glycated albumin therapy ameliorates early retinal microvascular pathology in db/db mice. *J Diabetes Complications* **1998**, *12*, 28-33.

101. Midena, E.; Segato, T.; Radin, S.; di Giorgio, G.; Meneghini, F.; Piermarocchi, S.; Belloni, A.S. Studies on the retina of the diabetic db/db mouse. I. Endothelial cell-pericyte ratio. *Ophthalmic Res* **1989**, *21*, 106-111.

102. Abid, M.R.; Guo, S.; Minami, T.; Spokes, K.C.; Ueki, K.; Skurk, C.; Walsh, K.; Aird, W.C. Vascular endothelial growth factor activates PI3K/Akt/forkhead signaling in endothelial cells. *Arteriosclerosis, thrombosis, and vascular biology* **2004**, *24*, 294-300. https://doi.org/10.1161/01.ATV.0000110502.10593.06.

103. Yun, J.H. Hepatocyte growth factor prevents pericyte loss in diabetic retinopathy. *Microvascular research* **2021**, *133*, 104103. https://doi.org/10.1016/j.mvr.2020.104103.